Article

ACTH modulates PTP-PEST activity and promotes its interaction with paxillin†

Alejandra Beatriz Gorostizaga[1], M Mercedes Mori Sequeiros Garcia[1], Andrea B Acquier[1,2], Juan J Lopez-Costa[3], Carlos F Mendez[1,2], Paula M Maloberti[1] and Cristina Paz[1*]

[1]Institute for Biomedical Research (INBIOMED), Department of Biochemistry, School of Medicine, University of Buenos Aires-CONICET, Buenos Aires, Argentina.
[2]Pharmacology Unit, School of Dentistry, University of Buenos Aires, Buenos Aires, Argentina.
[3]Institute of Cell Biology and Neurosciences "Prof. E. De Robertis", University of Buenos Aires-CONICET, Buenos Aires, Argentina.

Corresponding author:
*Dr Cristina Paz. Department of Biochemistry, School of Medicine, University of Buenos Aires, Paraguay 2155, 5th Floor (C1121ABG), Buenos Aires, Argentina. Tel.:+541145083672 ext. 36; Fax: +541145083672 ext. 31; e-mail address: crispaz1506@gmail.com.

Abbreviations:
Protein tyrosine phosphatases, PTPs; adrenocorticotropic hormone, ACTH; Poly (glutamic acid-tyrosine), pGT; cyclic adenosine mono-phosphate, cAMP; glyceraldehyde-3-phosphate dehydrogenase, GAPDH; protein kinase A, PKA.

Running head: ACTH modulates paxillin-PTP-PEST interaction

Keywords
- adrenal zona fasciculata
- ACTH
- protein tyrosine phosphatase
- paxillin
- phosphorylation

Grants
This work was supported in part by grants from the University of Buenos Aires (20020100100760 and 20020130100300) to CP and Consejo Nacional de Investigaciones Científicas y Técnicas, CONICET (PIP 112-200801-00209 and PIP 201101 00101) to CP. Cristina Paz holds a research position at CONICET.

Received 20 April 2015; Revised 31 March 2016; Accepted 4 April 2016
Journal of Cellular Biochemistry

DOI 10.1002/jcb.25566

Abstract

ACTH treatment has been proven to promote paxillin dephosphorylation and increase soluble protein tyrosine phosphatase (PTP) activity in rat adrenal *zona fasciculata* (ZF). Also, in-gel PTP assays have shown the activation of a 115-kDa PTP (PTP115) by ACTH. In this context, the current work presents evidence that PTP115 is PTP-PEST, a PTP that recognizes paxillin as substrate. PTP115 was partially purified from rat adrenal ZF and PTP-PEST was detected through Western blot in bioactive samples taken in each purification step. Immunohistochemical and RT-PCR studies revealed PTP-PEST expression in rat ZF and Y1 adrenocortical cells. Moreover, a PTP-PEST siRNA decreased the expression of this phosphatase. PKA phosphorylation of purified PTP115 isolated from non-ACTH-treated rats increased K_M and V_M. Finally, in-gel PTP assays of immunoprecipitated paxillin from control and ACTH-treated rats suggested a hormone-mediated increase in paxillin-PTP115 interaction, while PTP-PEST and paxillin co-localize in Y1 cells. Taken together, these data demonstrate PTP-PEST expression in adrenal ZF and its regulation by ACTH/PKA and also suggest an ACTH-induced PTP-PEST-paxillin interaction.

Introduction

Protein phosphorylation is an integral component of signal transduction pathways within eukaryotic cells and is regulated by the fine interplay of protein kinases and phosphatases. It has been established that protein tyrosine phosphatases (PTPs) play crucial roles in the regulation of many physiological and pathological processes (Hoekstra et al., 2012; Tautz et al., 2013
; Tonks, 2006). In particular, PTPs play critical roles in cell-matrix adhesion dynamics and cytoskeleton rearrangements which are relevant for cell migration (Hashemi et al., 2011; Jamieson et al., 2005; Rhee et al., 2014
). It is well documented that the exposure of steroidogenic cells in culture to the corresponding trophic hormones leads to a change in cell shape known as rounding-up. Adrenocorticotropic hormone (ACTH) is the main hormone regulating steroidogenesis and adrenal growth. Upon ACTH stimulation, adrenal cells rapidly increase steroid production (cortisol in human) through a mechanism that involves protein kinases, mainly cAMP-dependent protein kinase (protein kinase A, PKA) (Gallo-Payet, 2016). Han and Rubin established a link between tyrosine dephosphorylation and changes in cell shape in ACTH-stimulated cells (Han and Rubin, 1996). Specifically, they observed that the stimulation of Y1 adrenocortical cells with adrenocorticotropic hormone (ACTH) or with 8Br-cAMP –a permeable analog of the corresponding second messenger– rapidly produces a change in cell shape and promotes tyrosine dephosphorylation in cytosolic proteins. In addition, they observed that paxillin, a focal adhesion protein (Burridge et al., 1992), is maximally dephosphorylated in tyrosine residues upon cAMP stimulation even before this stimulus induces changes in cell shape. As both effects, i.e. changes in cell shape and paxillin dephosphorylation, are abrogated by protein tyrosine phosphatase inhibitors, these authors concluded that cAMP regulates paxillin phosphorylation status by eliciting an increase in tyrosine phosphatase activity, which in turn modulates cell shape.

Later, Vilgrain et al. showed the induction of paxillin dephosphorylation by ACTH also in bovine adrenocortical cells (Vilgrain et al., 1998). In addition, we demonstrated that *in vivo* ACTH treatment reduces phosphotyrosine content in proteins from rat adrenal *zona fasciculata* (ZF), one of them identified as paxillin, and produces a transient increase in tyrosine phosphatase activity in the cytosolic fraction (Paz et al., 1999). Moreover, *in vitro* incubation of adrenal ZF with 8Br-cAMP increases total tyrosine phosphatase activity, which suggests the presence of at least one PTP regulated by PKA-dependent phosphorylation events. Using an in-gel PTP activity assay, we showed that ACTH promotes the rapid activation of three PTPs in the cytosolic fraction of rat adrenal ZF, i.e. a 50-kDa, an 80-kDa and a 115-kDa PTP (PTP115) (Paz et al., 1999). Furthermore,

the fact that the luteinizing hormone also promotes PTP activation in MA-10 Leydig cells has lead us to propose that PTP action is an obligatory and common step in the cascade triggered by steroidogenic hormones. It has been demonstrated that SHP2, an 80-kDa tyrosine phosphatase, is required for full steroidogenesis (Cooke et al., 2011) and simultaneously modulates mitochondrial fusion and the localization of key steroidogenic proteins in the mitochondrion (Duarte et al., 2012). Paxillin is known to be a substrate of SHP2 and regulates cell motility in tumoral cells (Sausgruber et al., 2014). Thus, it is conceivable that, by acting on paxillin, SHP2 could contribute to modulating the actin cytoskeleton in order to promote mitochondrial subcellular distribution and fusion (Duarte et al., 2012). However, in several systems, paxillin has also been widely described as a substrate of PTP-PEST (Jamieson et al., 2005; Lu et al., 2006). PTP-PEST exhibits 86-kDa molecular weight, although it migrates as a 115-kDa protein in SDS-PAGE due to the presence of PEST sequences (proline, glutamate, serine and threonine-rich sequences) which alter its electrophoretic motility (Charest et al., 1995; Takekawa et al., 1992). Thus, this phosphatase could be the ACTH-activated enzyme of 115-kDa detected in adrenal ZF. Moreover, Western blot analyses of cytosolic proteins from rat adrenal ZF using an anti-PTP-PEST antibody have shown a weak reactive band migrating at 115-kDa. In this context, our hypothesis is that PTP115, which is activated by ACTH and PKA, and the reactive band detected by Western blot corresponds to the same protein, i.e. PTP-PEST. Therefore, our aim was to confirm the identity of PTP115 and characterize the effect of PKA on its enzymatic activity in a partially purified sample from rat adrenal ZF. We also analyzed the putative ACTH-mediated interaction of this phosphatase with paxillin.

Materials and Methods

Materials

ACTH was purchased from Elea Laboratories (Buenos Aires, Argentina). Poly (Glu:Tyr) or poly (glutamic acid-tyrosine) random copolymer (4:1 ratio), abbreviated as pGT, 8-bromo-adenosine 3,5-phosphate (8Br-cAMP), sodium orthovanadate, epidermal growth factor (EGF) fragment 20-31, insulin, insulin receptor, EGF receptor, PKA catalytic subunit from bovine heart, extravidin-peroxidase complex and bovine serum albumin (BSA), were purchased from Sigma (St. Louis, MO, USA). 9-Fluoro-11β, 17, 21-trihydroxy-16α-methylpregna-1,4-diene-3,20-dione (dexamethasone) was a kind gift from Ciba Geigy (Basel, Switzerland). Monoclonal anti-paxillin antibody was purchased from Transduction Laboratories (Lexington, KY, USA). Anti PTP-PEST antibody and Protein A/G Plus-Agarose were obtained from Santa Cruz Biotechnology, Inc. (Santa Cruz, CA, USA), whereas horseradish peroxidase-conjugated donkey anti-goat and goat anti-mouse secondary antibodies, as well as Immun-Blot polyvinylidene fluoride membrane were purchased from Bio-Rad

Laboratories (Hercules, CA, USA). The enhanced chemiluminescence kit Bio-Lumina was purchased from Kalium Technologies SRL (Bernal, Buenos Aires, Argentina). All other reagents were of the highest quality available.

Cell cultures

Murine Y1 adrenocortical tumor cells were generously provided by Dr. Bernard Schimmer (University of Toronto, Toronto, Canada). Y1 cells were grown in Ham-F10 medium, supplemented with 12.5% heat-inactivated horse serum and 2.5% heat-inactivated fetal bovine serum, 1.2 g/liter $NaHCO_3$, 200 IU/ml penicillin and 200 mg/ml streptomycin sulfate and maintained in a 5% CO_2 humidified atmosphere (Schimmer, 1979). The cultures were incubated with or without ACTH (25 nM) or 8Br-cAMP (500 μM) as stated in the legend of the corresponding figures. After treatments, total RNA or cell lysates were obtained.

RNA extraction and semiquantitative RT-PCR

Total RNA was isolated from Y1 cells using Tri-Reagent (MRC Carlsbad, CA) according to the manufacturer's instructions. The reverse transcription and PCR analyses were made using 2 μg of total RNA using random primers for reverse transcription (RT). The cDNAs generated were further amplified by PCR using the primers listed below. PTP-PEST forward, 5′-TTATCCCACAGCCACTGGAG-3′ and reverse, 5′-ATAGCACCTGTTCGTCCACA-3′ ; L19 forward, 5′-GAAATCGCCAATGCCAACTC-3′, and reverse, 5′ CTTAGACCTGCGAGCCTCA-3′. The reaction conditions for PTP-PEST were one cycle of 94 °C for 5 min, followed by 27 cycles of 94 °C for 30 sec, 53°C for 30 sec, and 72 °C for 60 sec. The reaction conditions for L19 were one cycle of 94 °C for 5 min, followed by 25 cycles of 94 °C for 30 sec, 55°C for 30 sec, and 72 °C for 30 sec. The number of cycles used was optimized for each gene to fall within the linear range of PCR amplification. PCR products were resolved on a 1.5% (wt/vol) agarose gel containing ethidium bromide. Gel images were obtained with a digital camera (Kodak Easy Share Z712 IS) and quantitated using the Gel-Pro-analyzer software (Media Cybernetics, LP, Silverspring. MD, USA) for windows. PCR results for each sample were normalized using L19 mRNA as an internal control.

RNA interference

A plasmid vector to express an small interfering RNA (siRNA)-targeting PTP-PEST was constructed as follows: a pair of 64-nucleotide (nt)-annealed DNA oligonucleotides was inserted between the BglII and HindIII restriction sites of the pSUPER.retro vector (OligoEngine) to express a short hairpin siRNA under the control of the polymerase-III H1-RNA promoter. A 19-nt target

sequence derived from murine PTP-PEST mRNA (accession NM_011203, 564-582 bp) was used. The set of 64-nt oligos containing this sequence is described below: sense, 5′-GATCCCCGACTACTTCATCCGAACACTT
CAAGAGAGTGTTCGGATGAAGTAGTCTTTTTA -3′ and antisense, 5′- GCTTAAAAAG ACTACTTCATCCGAACACTCTCTTGAAGTGTTCGGATGAAGTAGTCGGG-3′. Correct in-frame insertions were verified by sequencing.

Transfection assays

Cells were seeded the day before transfection, grown up to 80% confluence and transfected during 6 h using Lipofectamine 2000 reagent in Opti-MEM medium according to manufacturer's instructions (Invitrogen, Life Technologies, Inc.-BRL, Grand Island, NY, USA)

Animals

All animals were housed in groups in air-conditioned rooms, with lights on from 0700 to 1900, and given free access to laboratory chow and tap water. Studies were performed according to protocols evaluated and approved by the Animal Care and Use Committee (CICUAL) from the University of Buenos Aires, School of Medicine. Ninety-day-old female Wistar rats were used throughout. Adrenal glands were obtained from animals supplied with dexamethasone (10 µg/ml, *ad libitum*) in the drinking water for 16 h before sacrifice. Following dexamethasone treatment, animals were injected subcutaneously with 12,5 IU ACTH per kg of body weight (equivalent to 140 µg ACTH/kg) and killed 15 min later. Animals were decapitated and adrenal glands were removed, decapsulated and subjected to subcellular fractioning, as described below.

Subcellular fractioning

All subsequent steps were carried out at 5-8ºC. Adrenal glands were quartered and the quarters were gently homogenized in a glass tube with Teflon pestle in 0.2 ml per gland of an ice-cold buffer of 25 mM imidazole/HCl, pH 7.2, containing 230 mM mannitol, 70 mM sucrose and 0.1% 2-mercaptoethanol. For immunoprecipitation and Western blot analysis, homogenization was performed in the same buffer, this time containing 200 µM vanadate, 50 mM NaF and no 2-mercaptoethanol.

Nuclei and cellular debris were removed by centrifugation of the homogenate at 800xg for 10 min. Mitochondria were pelleted from the resulting supernatant by centrifugation at 9,000xg for 20 min. This post-mitochondrial supernatant was further centrifuged at 105,000xg for 60 min in order to obtain the cytosolic fraction.

Purification protocol

In order to obtain a sample of PTP115 with sufficient purity to analyze its kinetic parameters, we designed the following purification protocol. Cytosolic proteins of rat adrenal gland ZF were subjected to a purification protocol for PTP115, and fractions obtained in each purification step were analyzed by in-gel assay in order to select the fractions containing PTP115. First, cytosolic proteins were fractioned by precipitation with ammonium sulfate [$(NH_4)_2SO_4$] at 30, 50, 70 and 90% saturation (final concentration). After precipitation, proteins were dissolved in 20 mM imidazole buffer, pH 7.2, and the corresponding solutions were dialyzed for 18 h for salt removal in 50 mM imidazole and 0.05% 2-mercaptoethanol. After dialysis, an aliquot of each fraction was analyzed by in-gel PTP activity assay. The selected fractions were loaded on a DEAE-cellulose anion exchange column equilibrated with 20 mM imidazole, pH 7.2. The flow-through was collected and proteins were eluted with a discontinuous gradient of NaCl (100 to 400 mM). In-gel PTP assays revealed the highest PTP115 activity in fractions eluted with 400 mM NaCl. These samples were desalted and concentrated by centrifugation 1000xg for 15 min through a 100-kDa cut-off Centricon YM-100 (Millipore, Bedford MA, USA), a procedure that not only retains proteins over molecular weight cut-off but also removes salts and concentrates samples. A subsequent in-gel PTP activity assay revealed that the solution retained in the filter contained PTP115 and this sample was thus used for further experiments. The analysis of PTP-PEST by Western blot in samples selected in each purification step was carried out to confirm PTP115 identity.

PKA phosphorylation

A sample of purified PTP115 containing approximately 1.0 μg protein was separated in two equal aliquots and subjected to non-radioactive phosphorylation with or without 0.1 U PKA catalytic subunit for subsequent enzyme activity assays. Each reaction mixture (50 μl) contained the purified protein, 20 mM Tris-HCl, pH 7.4, 5 mM $MgCl_2$, 1 mM DTT and 50 μM ATP. Incubations were performed at 30°C for 15 min and stopped by dilution in a buffer containing 25 mM imidazole, pH 7.4, and 0.1% 2-mercaptoethanol (10- to 20-fold).

Preparation of PTP assay substrate ([^{32}P] pGT)

PTP activity was measured using [^{32}P] pGT as substrate. Labeling reactions were performed with [γ^{32}P]ATP and a kinase mixture containing EGF and insulin receptors, according to Burridge and Nelson's protocol (Burridge and Nelson, 1995). The reaction mixture contained 0.3 mg pGT in 0.17 ml of a buffer containing 150 mM NaCl, 2 mM $MnCl_2$, 12 mM magnesium acetate, 0.02% Triton X-100, 5% glycerol, 50 mM Hepes, pH 7.4, 0.1 mM ATP, 500 nM EGF, 1 mM insulin, 2.5 U EGF-receptor, 17.5 U insulin receptor and 0.125 mCi ATP. The reaction was allowed to proceed

for 16 h and then stopped by adding an equal volume of 20% trichloroacetic acid (TCA). After 30 min on ice, the sample was centrifuged at 12,000xg for 10 min at 4ºC. This pellet was dissolved in 100 µl of 2 mM Tris, pH 8, and loaded on a G50 Sephadex column equilibrated with 50 mM imidazole, pH 7.2. The elution was performed with the same buffer and fractions of 0.4 ml were collected. The incorporation of ^{32}P was measured by scintillation counting in order to select the appropriate fraction.

Total PTP activity measurement

After *in vitro* phosphorylation of purified PTP115, the kinetic parameters of the enzyme were evaluated measuring PTP activity as described by Tonks et al. (Tonks and Neel, 1996). Briefly, the samples (10-25 ng) were incubated with [^{32}P] pGT (radioactivity 5.000-100.000 cpm/tube) and a buffer containing 25 mM imidazole, pH 7.4, 0.1% 2-mercaptoethanol, 1 mg/ml BSA in a 60 µl reaction volume. The reactions were allowed to proceed for 10 min at 30ºC and then stopped by adding 180 µl ice-cold 20% TCA and 20 µl of 25 mg/ml BSA as input to facilitate subsequent precipitation. After incubation for 5 min at 4°C, 5-min centrifugation was conducted at 12,000xg to separate the protein precipitated from the supernatant containing Pi. Subsequently, 200 µl supernatant was transferred to a tube for radioactivity quantification in a scintillation counter. Dephosphorylation was linear with respect to time and enzyme concentration up to 50% [^{32}P] released. Radioactivity in samples without enzyme (blank) was routinely less than 5% of total [^{32}P] in the assay.

In-gel PTP activity assay

An in-gel PTP activity assay, using [^{32}P]pGT as substrate, was used to follow PTP115 through the purification process. An amount of $5x10^5$ cpm of [^{32}P]pGT/ml was incorporated into the regular polyacrylamide gel mixture prior to polymerization. SDS/polyacrylamide gel electrophoresis was performed as described by Laemmli (Laemmli, 1970) on 10% acrylamide gels. PTP activity was detected in-gel, following the procedure described by Burridge and Nelson (Burridge and Nelson, 1995). Briefly, after sample separation by electrophoresis (5-10 µg of protein per lane), SDS was removed and the gel was incubated in different buffers for protein renaturation inside the gel. The washing solutions and conditions used were: a) 20% isopropanol, 50 mM Tris HCl, pH 8, 5-16 h; b) 0.3% 2-mercaptoethanol, 50 mM Tris HCl, pH 8, 30 min twice; c) 1 mM EDTA, 6 M guanidine chloride, 50 mM Tris HCl, pH 8 (denaturation buffer), 90 min; d) 1 mM EDTA, 0.3% 2-mercaptoethanol, 0.04% Tween 20, 50 mM Tris HCl, pH 8, 1h three times; d) the same solution as

in c), including 4 mM dithiothreitol, 5-16 h. After washing, the gels were dyed with Coomassie blue and dried before exposure to X-ray film.

Immunohistochemistry

Tissue processing

Rats were anaesthetized with chloral hydrate (350 mg/kg) and perfused transcardially with a solution containing 4% paraformaldehyde (PFA) in 0.1M phosphate buffer. Adrenal glands were dissected out and postfixed by immersion in the same fixative solution for 2h. After cryoprotection in a solution containing 30% sucrose, adrenal glands were cut using a Lauda Leitz cryostat. The sections (thickness 20 microns) were mounted on gelatin-coated glass slides and processed for immunohistochemistry.

Immunohistochemical method

Cryostat sections were incubated in 10% normal horse serum for 1h at room temperature in order to avoid unspecific staining and then incubated overnight in goat PTP-PEST antibody (1:500) at 4°C. The following day sections were incubated in donkey anti-goat biotinylated antibody (Jackson ImmunoResearch Laboratories Inc, Baltimore, PA, USA; 1:125) and in extravidin-peroxidase complex (1:200). All antisera were diluted in phosphate buffered saline (PBS) containing 0.2% Triton X-100. Incubations with biotinylated antibody and extravidin-peroxidase complex were performed at room temperature for 1h. The reaction was developed using the DAB/nickel intensification procedure (Hancock, 1984).

Western blot

After the appropriate treatments, proteins were subjected to Western blot analysis. Proteins were separated by 10% SDS–PAGE, as described by Laemmli (Laemmli, 1970), and transferred onto polyvinylidene difluoride membranes (PVDF). Immunoblotting was performed using anti-goat polyclonal PTP-PEST antibody (1:1,000). Bound antibodies were developed by incubation with horseradish peroxidase-conjugated secondary antibody (donkey anti-goat). Immunoreactive bands were detected using an enhanced chemiluminescence kit.

Immunoprecipitation

Cytosolic proteins (400 μg) isolated from ACTH-treated and non-treated (control) rat adrenal gland ZF were incubated overnight at 4-8ºC with 4 μg monoclonal anti-paxillin IgG or 4 μg polyclonal PTP-PEST antibody and 20 μl protein A/G Plus-Agarose in a final volume of 0.5 ml in the following immunoprecipitation buffer: 10 mM Tris, pH 7.4, 150 mM NaCl, 1 mM EDTA, 1 mM

EGTA, 1% Triton X-100, 0.5% Nonidet P40, 200 mM sodium orthovanadate, 50 mM NaF, 1 mM phenylmethylsulfonyl fluoride (PMSF) and 10 mM leupeptin (Paz et al., 1999). A sample from ACTH-treated rats was immunoprecipitated in the absence of paxillin antibody as control. After incubation, samples were centrifuged at 12,000xg for 4 min and the pellets obtained were washed four times with 0.5 ml of immunoprecipitation buffer prior to boiling in SDS loading buffer. The samples obtained were analyzed by in-gel PTP activity assay and Western blot.

Immunofluorescence

Y1 cells were grown to approximately 60% confluence on poly-l-lysine glass coverslips. After treatments, cells were fixed with 4% PFA in PBS for 10 min at room temperature and permeabilized with blocking solution (0.3% Triton X-100, 1% albumin in PBS) for 60 min at room temperature. Cells were incubated overnight at 4°C with primary antibodies anti-PTP-PEST polyclonal IgG (1:500) and anti-paxillin monoclonal IgG (1:500). After thorough washing, cells were incubated for 1 h at room temperature with secondary antibodies Cy3-conjugated goat anti-mouse (red, paxillin; 1:1000) and Cy2-conjugated donkey anti-goat (green, PTP-PEST; 1:1000). Nuclei were stained with 4′,6-diamidino-2-phenylindole (DAPI). Coverslips were mounted onto the slides using Calbiochem Fluorsave anti-fade reagent (Merck-Millipore, Billerica, MA, USA). For confocal analysis, images were taken using an Olympus FV300 microscope.

Protein determination

Protein concentration was determined by the method described by Bradford (Bradford, 1976) using BSA as standard.

Results

Immunodetection of PTP-PEST in rat adrenal gland

Immunohistochemical analyses were conducted in order to establish whether PTP-PEST is expressed in rat adrenal gland ZF. Intense immunoreactivity was detected throughout ZF, whereas weak immunostaining was observed in ZG (Fig. 1, A). In ZF, immunostaining was localized mostly in the cytoplasm, while nuclei were devoid of signal (Fig. 1, B and C).

Detection of PTP-PEST mRNA in rat adrenal ZF and Y1 adrenocortical cells

Next, PTP-PEST mRNA levels were evaluated in adrenal ZF from ACTH-treated rats at different times post-injection. PTP-PEST messenger levels were also analyzed in Y1 cells, a mouse

adrenocortical cell line, incubated with ACTH for the indicated times. Total RNA from rat adrenal ZF or Y1 cells was subjected to semi-quantitative RT-PCR analysis using specific oligonucleotides for PTP-PEST, and PCR products were analyzed on agarose gel with ethidium bromide. In both samples, fragments isolated exhibited the size expected for PTP-PEST (Fig. 2). The identity of the amplified products was confirmed by sequencing (Macrogen Korea, Geumcheon-gu, Seoul, Rep. of Korea). Similar results were obtained in MA-10 Leydig cells (data not shown). Moreover, no changes in PTP-PEST mRNA levels were observed after ACTH stimulation.

Partial purification of PTP115

A purification protocol was designed to obtain a sample of PTP115 essentially free of other tyrosine phosphatases and study its kinetic parameters. A commercial PTP-PEST antibody was used for Western blot analyses of the fractions selected throughout the procedure, in an attempt at identifying PTP115. PTP115 was precipitated with 30% and, mostly, with 50% $(NH_4)_2SO_4$, although this fraction also contained a large amount of other tyrosine phosphatases (Fig. 3, A). Given our interest in obtaining a sample of PTP115 mostly devoid of other PTPs in order to determine enzyme kinetic parameters, we selected the fraction precipitated with 30% $(NH_4)_2SO_4$ for chromatography on a DEAE-cellulose anion-exchange column. The fraction eluted with 400 mM NaCl retained PTP115 activity and contained relatively small amounts of other PTPs (Fig. 3, B, lane 4), which is why it was chosen for the next step, i.e. filtration through Centricon YM-100 (100-kDa pore size). This procedure removed NaCl used in the elution of the DEAE column, concentrated the sample and excluded proteins under 100-kDa molecular weight (Fig 3, C, lane 4). Western blot analyses of PTP-PEST were conducted in cytosolic proteins, proteins present in the fraction precipitated with 30% $(NH_4)_2SO_4$, in the 400 mM NaCl eluate and in the solution retained in the filter (Fig. 3, D, lanes 1-4, respectively). The purification protocol yielded approximately 0.5-1.5 μg protein mixture enriched in PTP115 starting from 30-60 mg cytosolic proteins, according to the results of at least five experiments. Table 1 shows protein amounts recovered in the fractions selected along purification in a typical process of purification which rendered between 0.5 and 1 μg of partially purified PTP115 starting from 38 mg cytosolic proteins. Similar results were obtained in at least four additional purification processes.

Effect of PKA phosphorylation on enzyme kinetic parameters

The activity of purified PTP115 phosphorylated *in vitro* in the presence or absence of PKA was evaluated using different concentrations of substrate, and the reaction rate was expressed as pmoles of ^{32}P released/min/μg enzyme. Lineweaver-Burk analysis of data showed that PKA phosphorylation increased both the apparent K_M (~3-fold) and V_{max} of PTP115 (~1.6-fold, Fig. 4).

Analysis of PTP-PEST-paxillin interaction

To analyze the putative ACTH-induced interaction of PTP-PEST and paxillin, cytosolic proteins obtained from rats treated with ACTH or vehicle were immunoprecipitated using an anti-paxillin antibody. Analysis of cytosolic proteins by in-gel PTP assays revealed a band of activity corresponding to a 115 kDa protein, not only in samples from ACTH-treated rats but also in samples from non-treated rats (control) (Fig. 5, A, left). These samples were used for immunoprecipitation assays. Corresponding immunoprecipitates were then separated in two aliquots: one of them was analyzed by in-gel PTP assay and the other one by Western blot. In-gel PTP assay revealed a band corresponding to a 115 kDa protein in immunoprecipitates from ACTH-treated rats, meanwhile in samples from control rats PTP activity was undetectable (Fig. 5, A, right). Western blot analysis showed similar amounts of paxillin in immunoprecipitates from control or ACTH-treated rats (Fig. 5, B). In addition, in-gel PTP assay of immunoprecipitates from ACTH-treated rats revealed only a band corresponding to a 115 kDa protein. This band was absent in the immunoprecipitates obtained in the absence of the specific antibody (Fig. 5, C). We also analyzed by Western blot the presence of PTP-PEST in paxillin immunoprecipitated (data not shown). However, PTP-PEST was not detected in these samples, perhaps due to the low amount of PTP-PEST co-immunoprecipitated with paxillin.

Confocal microscopy analysis shows the localization of PTP-PEST and paxillin in control and in cells exposed to ACTH (Fig. 6). In non-stimulated Y1 cells, PTP-PEST exhibited cytoplasmic labeling, as evidenced by immunocytochemical analyses, while paxillin was localized at discrete sites in the periphery of the cells, near the plasma membrane, resembling focal adhesions. In turn, hormonal stimulation of the cells promoted morphological changes and focal adhesion disassembly as previously described. As a novel finding, PTP-PEST was observed to colocalize with paxillin in the cytoplasmic region (Fig. 6, A). DAPI staining confirmed PTP-PEST cytoplasmic localization (Fig.6, B).

Down-regulation of PTP-PEST expression by an specific siRNA

Finally, in order to confirm the expression of PTP-PEST in adrenal cells, we designed a short hairpin small interfering RNA (siRNA) to down-regulate this protein. Y1 cells were transiently transfected with a vector carrying the sequence encoding the siRNA or the empty vector and incubated with or without ACTH for 30 min. PTP-PEST mRNA levels in cells expressing siRNA were lower than in cells carrying the empty vector both in control and ACTH-treated cells (Fig. 7, A). The partial reduction in mRNA levels (35%) obtained by siRNA expression was congruent with

the efficiency of the transfection. In addition, the siRNA also decreased PTP-PEST protein levels (Fig. 7, B). Thus, these results confirm the expression of PTP-PEST in adrenocortical cells.

Discussion

PTPs have been widely implicated in ACTH-stimulated steroidogenesis (Paz et al., 1999) and hormone-dependent mitochondrial dynamics (Duarte et al., 2012). In addition, we have previously demonstrated that ACTH promotes paxillin dephosphorylation and the activation of three PTPs in adrenal gland ZF, one of them of 115-kDa (PTP115) As its most relevant aspects, the present work provides strong evidence that PTP115 is PTP-PEST, shows that the kinetic parameters of PTP115 – isolated from ZF of non-stimulated rats– are modified by PKA-mediated phosphorylation, and suggests a PTP-PEST-paxillin interaction. Moreover, the current findings also suggest that ACTH increases this interaction.

PTP-PEST was detected in adrenal ZF and in Y1 cell by Western blot analysis. Moreover PTP-PEST expression was confirmed by a siRNA against PTP-PEST. A direct identification of PTP115 could have been performed by in-gel PTP analyses of cytosolic proteins immunodepleted of PTP-PEST. However, as the commercial antibody available is not suitable for immunoprecipitation assays, the approach used for the identification consisted in the recognition of PTP-PEST by Western blot in the bioactive samples selected in each purification step. In addition, immunohistochemical analyses demonstrated the presence of PTP-PEST in rat adrenal gland, almost exclusively in ZF, while RT-PCR assays revealed the presence of PTP-PEST mRNA. Moreover, in gel-PTP analyses of adrenocortical Y1 cell lysates also rendered a 115-kDa bioactive band (data not shown) and, in line with these results, Y1 cells expressed PTP-PEST mRNA and protein. Taken together, these results strongly suggest that PTP115 is PTP-PEST. Several PTPs are phosphoproteins *in vivo*, which suggests the potential of reversible phosphorylation as a mechanism to control enzymatic activity. Accordingly, potato acid phosphatase treatment of ZF soluble proteins obtained from ACTH-stimulated rats reduces the activity of PTP115 to control levels, which indicates that this protein, identified as PTP-PEST in this work, is activated by phosphorylation (Paz et al., 2000). It has been previously demonstrated that PTP-PEST is phosphorylated *in vivo* by PKA, PKC and ERK (Garton and Tonks, 1994; Zheng and Lu, 2013). *In vitro* phosphorylation of recombinant PTP-PEST by PKA occurs predominantly in Ser39 and Ser435, in the catalytic and non-catalytic domain, respectively. Ser39 phosphorylation has been found to inhibit enzymatic activity due to a decrease in PTP-PEST affinity for the substrate (phosphorylated RCM-lyzosime), while Ser435 phosphorylation has no effects on enzymatic activity (Garton and Tonks, 1994). Since this site is involved in protein degradation (Garton and Tonks, 1994), this modification could have a

role in protein stability. ERK1/2 has also been reported to phosphorylate PTP-PEST, particularly at Ser571 (Zheng and Lu, 2013). PIN1, a peptidyl prolyl *cis/trans* isomerase, is able to recognize PTP-PEST phosphorylated specifically at this site and promote its isomerization. As a consequence, an increase is observed in the interaction of PTP-PEST and the substrate, focal adhesion kinase (FAK) (Zheng et al., 2011).

The present data show that *in vitro* PKA phosphorylation of purified PTP-PEST isolated from adrenal gland ZF from non-stimulated rats increases the apparent K_M for synthetic substrate pGT, as reported for phosphorylated RCM-lyzosime (Garton and Tonks, 1994). The incorporation of a negatively charged group in a residue such as Ser39, which is near PTP-PEST catalytic domain, has been previously proposed to hinder enzyme-substrate binding. Therefore, even if site identification is beyond the scope of our work, it is probable that PKA phosphorylation of PTP-PEST from adrenal gland ZF occurs at Ser39, which displays the highest phosphorylation probability (score 0.997, NetPhos 2.0 Server).

The present study also shows that *in vitro* phosphorylation of PTP-PEST from ZF adrenal gland produces an increase in V_M, in contrast with the conclusion reached by Garton and Tonks, who report that PKA phosphorylation does not substantially modify V_M (Garton and Tonks, 1994). Moreover, the effect of PKA phosphorylation on PTP-PEST activity described in this work is in contrast with the effect reported for Ser/Tre kinase MST3 phosphorylation, i.e. the inhibition or PTP-PEST enzymatic activity (Lu et al., 2006). Although no conclusive explanations can be given yet for these discrepancies, the possibility remains that *in vitro* phosphorylation, in addition to the putative basal phosphorylation of purified PTP-PEST, could lead to enzyme activation. Furthermore, the fact that PTP-PEST presents consensus sites for several protein kinases provides support for this hypothesis.

As mentioned above, isomerase PIN1 specifically recognizes Ser571-phosphorylated PTP-PEST and modifies its conformation, which facilitates enzyme-substrate interaction. However, whether a similar ACTH-activated mechanism is working in our system remains elusive. In this context, it is worth mentioning that ACTH triggers the activation of not only PKA and PKC but also MAPK family members such as ERK1/2 (Zheng and Lu, 2013), which could participate in the *in vivo* regulation of PTP-PEST. In this context, we have analyzed the putative regulation of paxillin-PTP-PEST interaction by ACTH. Indeed, the present data suggest an stimulatory effect of ACTH on this interaction, since in-gel PTP assay shows that a PTP of 115 kDa is co-immunoprecipitated with paxillin just in samples from ACTH-treated rats. However, Western blot analysis fails to detect PTP-PEST in the immunoprecipitates obtained with the anti-paxillin antibody. According to the yield of purification, there is a low amount of PTP-PEST in cytosolic proteins from adrenal gland, suggesting that the low amount of PTP-PEST co-immunoprecipitated is undetectable by Western

blot. Nevertheless, the fact that using an antibody against paxillin only one PTP –which correspond to a 115 kDa protein– is co-immunoprecipitated and that this co-immunoprecipitation is only observed in samples from ACTH-treated rats suggests an stimulatory effect of ACTH on paxillin-PTP-PEST interaction rather than on PTP115 activity.

The findings reported here raise the issue of the physiological role of ACTH-regulated PTP-PEST-paxillin interaction and paxillin dephosphorylation in the adrenal cortex. In this context, PTP-PEST-paxillin interaction could contribute to mitochondrial dynamics, thus having a role in steroidogenesis. Indeed, mitochondrial fusion is an essential event in hormonal stimulation of steroidogenesis (Duarte et al., 2012), while paxillin dephosphorylation could modulate actin cytoskeleton reorganization to facilitate this fusion (Duarte et al., 2012). It is largely established that PTP-PEST regulates cell spreading and migration through dephosphorylation of focal adhesion proteins (Jamieson et al., 2005). Therefore, PTP-PEST activation and paxillin dephosphorylation by ACTH might also play a role in cell migration associated with adrenal gland growth and zonation. Indeed, it is recognized that cell division is mostly confined to stem cells located in the outer cortex, where ACTH promotes not only cell division but also medulla-bound movement and terminal differentiation (Lu et al., 2006).

In summary, our work identifies the expression of PTP-PEST in adrenal ZF and strongly suggests that the ACTH-activated PTP115 is PTP-PEST. The effect of *in vitro* PKA phosphorylation of the enzyme isolated from non-ACTH-treated rats resembles the effect produced by *in vivo* ACTH treatment, which suggests that this hormone activates PTP-PEST by phosphorylation. The modulation of PTP-PEST and paxillin by ACTH could thus contribute to the action of this hormone on steroidogenesis and/or adrenal growth.

Bibliography

Bradford, M.M. 1976. A rapid and sensitive method for the quantitation of microgram quantities of protein utilizing the principle of protein-dye binding. *Anal Biochem*. 72:248-54.

Burridge, K., and A. Nelson. 1995. An in-gel assay for protein tyrosine phosphatase activity: detection of widespread distribution in cells and tissues. *Anal Biochem*. 232:56-64.

Burridge, K., L.A. Petch, and L.H. Romer. 1992. Signals from focal adhesions. *Curr Biol*. 2:537-9.

Cooke, M., U. Orlando, P. Maloberti, E.J. Podesta, and F. Cornejo Maciel. 2011
Tyrosine phosphatase SHP2 regulates the expression of acyl-CoA synthetase ACSL4. *J Lipid Res*. 52:1936-48.

Charest, A., J. Wagner, S.H. Shen, and M.L. Tremblay. 1995. Murine protein tyrosine phosphatase-PEST, a stable cytosolic protein tyrosine phosphatase. *Biochem J*. 308 (Pt 2):425-32.

Duarte, A., C. Poderoso, M. Cooke, G. Soria, F. Cornejo Maciel, V. Gottifredi, and E.J. Podesta. 2012. Mitochondrial fusion is essential for steroid biosynthesis. *PLoS One*. 7:e45829.

Gallo-Payet, N. 2016. Adrenal and extra-adrenal functions of ACTH. *J Mol Endocrinol*.

Garton, A.J., and N.K. Tonks. 1994. PTP-PEST: a protein tyrosine phosphatase regulated by serine phosphorylation. *Embo J*. 13:3763-71.

Han, J.D., and C.S. Rubin. 1996. Regulation of cytoskeleton organization and paxillin dephosphorylation by cAMP. Studies on murine Y1 adrenal cells. *J Biol Chem*. 271:29211-5.

Hancock, M.B. 1984. Visualization of peptide-immunoreactive processes on serotonin-immunoreactive cells using two-color immunoperoxidase staining. *J Histochem Cytochem*. 32:311-4.

Hashemi, H., M. Hurley, A. Gibson, V. Panova, V. Tchetchelnitski, A. Barr, and A.W. Stoker. 2011. Receptor tyrosine phosphatase PTPgamma is a regulator of spinal cord neurogenesis. *Mol Cell Neurosci*. 46:469-82.

Hoekstra, E., M.P. Peppelenbosch, and G.M. Fuhler. 2012. The role of protein tyrosine phosphatases in colorectal cancer. *Biochim Biophys Acta*. 1826:179-88.

Jamieson, J.S., D.A. Tumbarello, M. Halle, M.C. Brown, M.L. Tremblay, and C.E. Turner. 2005. Paxillin is essential for PTP-PEST-dependent regulation of cell spreading and motility: a role for paxillin kinase linker. *J Cell Sci*. 118:5835-47.

Laemmli, U.K. 1970. Cleavage of structural proteins during the assembly of the head of bacteriophage T4. *Nature*. 227:680-5.

Lu, T.J., W.Y. Lai, C.Y. Huang, W.J. Hsieh, J.S. Yu, Y.J. Hsieh, W.T. Chang, T.H. Leu, W.C. Chang, W.J. Chuang, M.J. Tang, T.Y. Chen, T.L. Lu, and M.D. Lai. 2006. Inhibition of cell migration by autophosphorylated mammalian sterile 20-like kinase 3 (MST3) involves paxillin and protein-tyrosine phosphatase-PEST. *J Biol Chem*. 281:38405-17.

Paz, C., F. Cornejo MacIel, C. Mendez, and E.J. Podesta. 1999. Corticotropin increases protein tyrosine phosphatase activity by a cAMP-dependent mechanism in rat adrenal gland. *Eur J Biochem*. 265:911-8.

Paz, C., F. Cornejo Maciel, C. Poderoso, A. Gorostizaga, and E.J. Podesta. 2000. An ACTH-activated protein tyrosine phosphatase (PTP) is modulated by PKA-mediated phosphorylation. *Endocr Res*. 26:609-14.

Rhee, I., M.C. Zhong, B. Reizis, C. Cheong, and A. Veillette. 2014
Control of dendritic cell migration, T cell-dependent immunity, and autoimmunity by protein tyrosine phosphatase PTPN12 expressed in dendritic cells. *Mol Cell Biol*. 34:888-99.

Sausgruber, N., M.M. Coissieux, A. Britschgi, J. Wyckoff, N. Aceto, C. Leroy, M.B. Stadler, H. Voshol, D. Bonenfant, and M. Bentires-Alj. 2014. Tyrosine phosphatase SHP2 increases cell motility in triple-negative breast cancer through the activation of SRC-family kinases. *Oncogene*.

Schimmer, B.P. 1979. Adrenocortical Y1 cells. *Methods Enzymol*. 58:570-4.

Takekawa, M., F. Itoh, Y. Hinoda, Y. Arimura, M. Toyota, M. Sekiya, M. Adachi, K. Imai, and A. Yachi. 1992. Cloning and characterization of a human cDNA encoding a novel putative cytoplasmic protein-tyrosine-phosphatase. *Biochem Biophys Res Commun*. 189:1223-30.

Tautz, L., D.A. Critton, and S. Grotegut. 2013

Protein tyrosine phosphatases: structure, function, and implication in human disease. *Methods Mol Biol*. 1053:179-221.

Tonks, N.K. 2006. Protein tyrosine phosphatases: from genes, to function, to disease. *Nat Rev Mol Cell Biol*. 7:833-46.

Tonks, N.K., and B.G. Neel. 1996. From form to function: signaling by protein tyrosine phosphatases. *Cell*. 87:365-8.

Vilgrain, I., A. Chinn, I. Gaillard, E.M. Chambaz, and J.J. Feige. 1998. Hormonal regulation of focal adhesions in bovine adrenocortical cells: induction of paxillin dephosphorylation by adrenocorticotropic hormone. *Biochem J*. 332 (Pt 2):533-40.

Zheng, Y., and Z. Lu. 2013. Regulation of tumor cell migration by protein tyrosine phosphatase (PTP)-proline-, glutamate-, serine-,and threonine-rich sequence (PEST). *Chin J Cancer*. 32:75-83.

Zheng, Y., W. Yang, Y. Xia, D. Hawke, D.X. Liu, and Z. Lu. 2011

Ras-induced and extracellular signal-regulated kinase 1 and 2 phosphorylation-dependent isomerization of protein tyrosine phosphatase (PTP)-PEST by PIN1 promotes FAK dephosphorylation by PTP-PEST. *Mol Cell Biol*. 31:4258-69.

Table 1: Purification of PTP115 from rat adrenal ZF. Purification was carried out as described in Materials and Methods. The table shows the data of a representative purification process performed at least five times.

Figure legends

Figure 1. Detection of PTP-PEST in rat adrenal gland. Tissue sections were treated for the detection of PTP-PEST as described in Materials and Methods. **A,** PTP-PEST immunoreactivity in adrenal gland (10X); **B,** PTP-PEST immunoreactivity in ZF (40X); **C,** PTP-PEST immunoreactivity in ZF (magnified), where arrows show nuclei (white) and cytoplasm (black).

Figure 2. Detection of PTP-PEST mRNA in rat adrenal ZF and Y1 adrenocortical cells. Semiquantitative RT-PCR assays of PTP-PEST mRNA were carried out with L19 mRNA as loading control. **A,** adrenal ZF from rats treated with ACTH (12,5 IU/kg weight); **B**, Y1 mouse adrenocortical cells exposed to ACTH (25 nM). PCR products were resolved on agarose gels with ethidium bromide and the optical density of each band was quantified. Normalized PTP-PEST mRNA values are expressed in arbitrary units. Each panel shows a representative gel and the quantitative representation of normalized data expressed as the mean ± SEM of four independent experiments. Data were analyzed by ANOVA.

Figure 3: Partial purification and identification of PTP115. Aliquots from the different fractions obtained in each purification step were analyzed by in-gel PTP activity assay (5-10µg). For A, B and C, autoradiography is shown on the left and gel Coomassie blue staining on the right. **A,** cytosolic and $(NH_4)_2SO_4$-precipitated proteins (30-90%); **B,** aliquot of proteins precipitated with 30% $(NH_4)_2SO_4$ (lane 1), proteins eluted during loading sample onto DEAE-cellulose anion exchange column (lane 2) and proteins present in fractions eluted with 100 mM (lane 3) and 400 mM NaCl (lane 4); **C,** proteins present in the cytosolic fraction (lane 1), in the fractions selected from $(NH_4)_2SO_4$ precipitation and anion-exchange chromatography (lanes 2 and 3, respectively), and in the sample retained in a 100-kDa Centricon YM tube (lane 4); **D,** detection of PTP-PEST by Western blot in the cytosolic fraction (lane 1), in the 30% $(NH_4)_2SO_4$ precipitate (lane 2), in the 400-mM NaCl eluate (lane 3) and in the solution retained in the Centricon tube (lane 4).

Figure 4: Lineweaver-Burk analysis of PTP115. Partially purified PTP115 was phosphorylated *in vitro* in the presence or absence of PKA. Phosphatase activity of appropriate aliquots of the phosphorylation reaction mixtures was evaluated using different amounts of [^{32}P] pGT. The results illustrated are the means from duplicate assays and are plotted as the reciprocal of enzyme activity (pmoles^{32}P released/min/µg enzyme) versus the reciprocal of substrate amount (cpm [^{32}P] pGT). The study was performed twice with similar results.

Figure 5: PTP-PEST-paxillin interaction. Cytosolic proteins obtained from rats treated with ACTH or vehicle (C) were immunoprecipitated using an anti-paxillin antibody. Each sample containing the immunoprecipitated proteins was separated in two aliquots for **A,** in-gel PTP activity assays and **B,** Western blot analysis of paxillin. **C**, whole lanes corresponding to the analysis by in-gel PTP assay of immunoprecipitated from cytosolic proteins isolated from ACTH-treated rats with and without anti-paxillin antibody. The figure shows representative images of three independent experiments

Figure 6: PTP-PEST-paxillin colocalization. A: ACTH-treated or non-treated Y1 adrenocortical cells were immunostained using antibodies against PTP-PEST and paxillin. PTP-PEST was stained in green and paxillin was stained in red using Cy2 and Cy3-conjugated secondary antibodies,

respectively. **B**: ACTH-treated or non-treated Y1 adrenocortical cells were immunostained using PTP-PEST antibody (green) and DAPI.

Figure 7: Effect of a siRNA-targeting PTP-PEST on PTP-PEST mRNA and protein levels. Y1 adrenocortical cells were transiently transfected with pSUPER.retro-PTP-PEST (PTP-PEST siRNA) or the empty expression vector (Mock) as indicated. After that, cells were incubated in the absence (Control) or presence of ACTH (25 nM) for 30 min. After that: cells were harvested and total RNA (A) or total cell lysates (B) were obtained. Total RNA was subjected to RT-PCR with specific primers for PTP-PEST and L19 cDNA as loading control. Cell lysates were analyzed by Western blot using an antibody against PTP-PEST and β tubulin as loading control. Each panel shows a representative gel and the quantitative representation of normalized data expressed as the mean ± SEM of three independent experiments. * $P<0.05$, ** $P<0.01$ vs. mock-transfected cells by ANOVA followed by Tukey´s test.

Table 1

Fraction	Proteins (µg)	Specific activity (UA/µg)
Cytosol	38,000	1
30 % saturation $(NH_4)_2SO_4$	749	12
Eluate from DEAE column 400 mM NaCl	80	39
Solution retained on the Amicon filter	< 0.5	6100

Figure 1

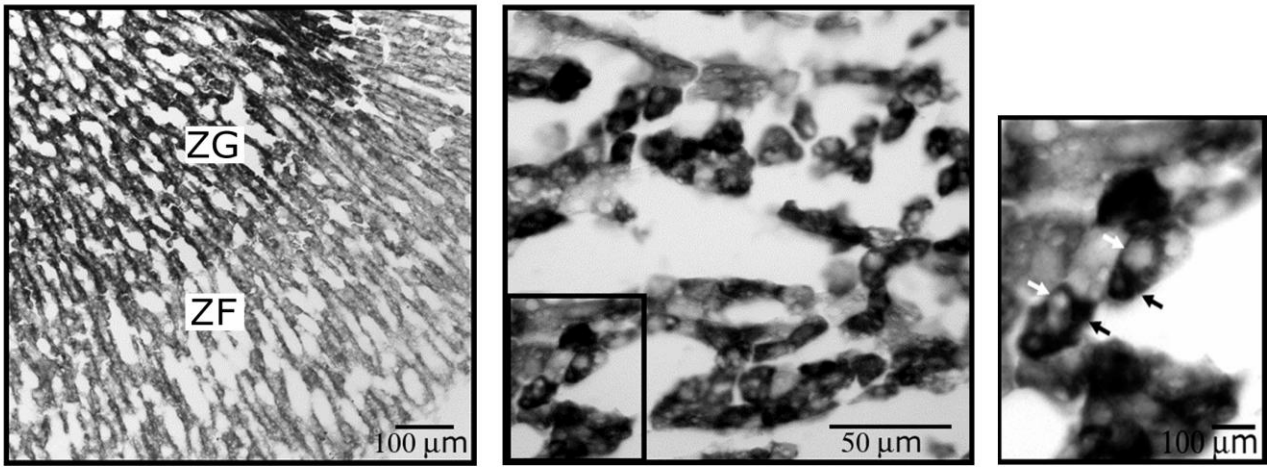

A **B** **C**

Figure 2

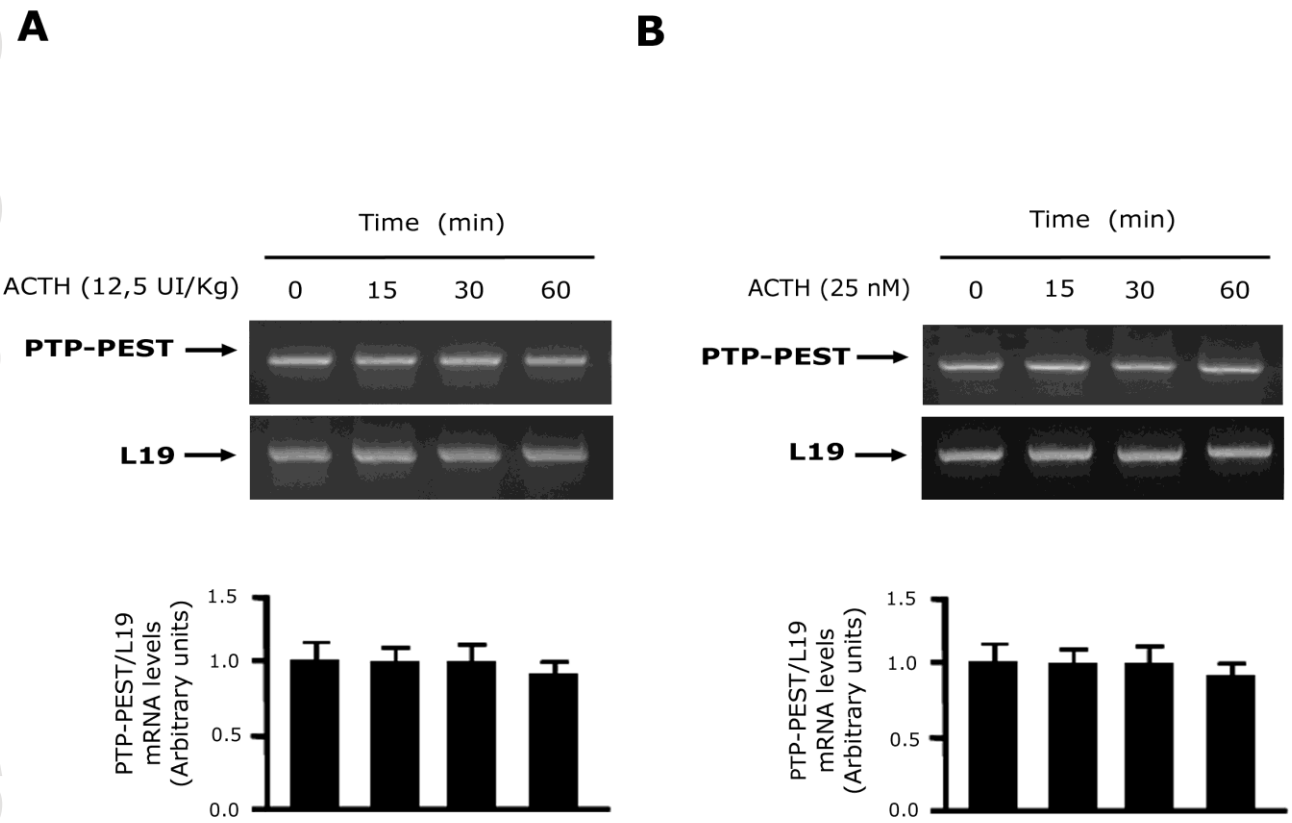

Figure 3

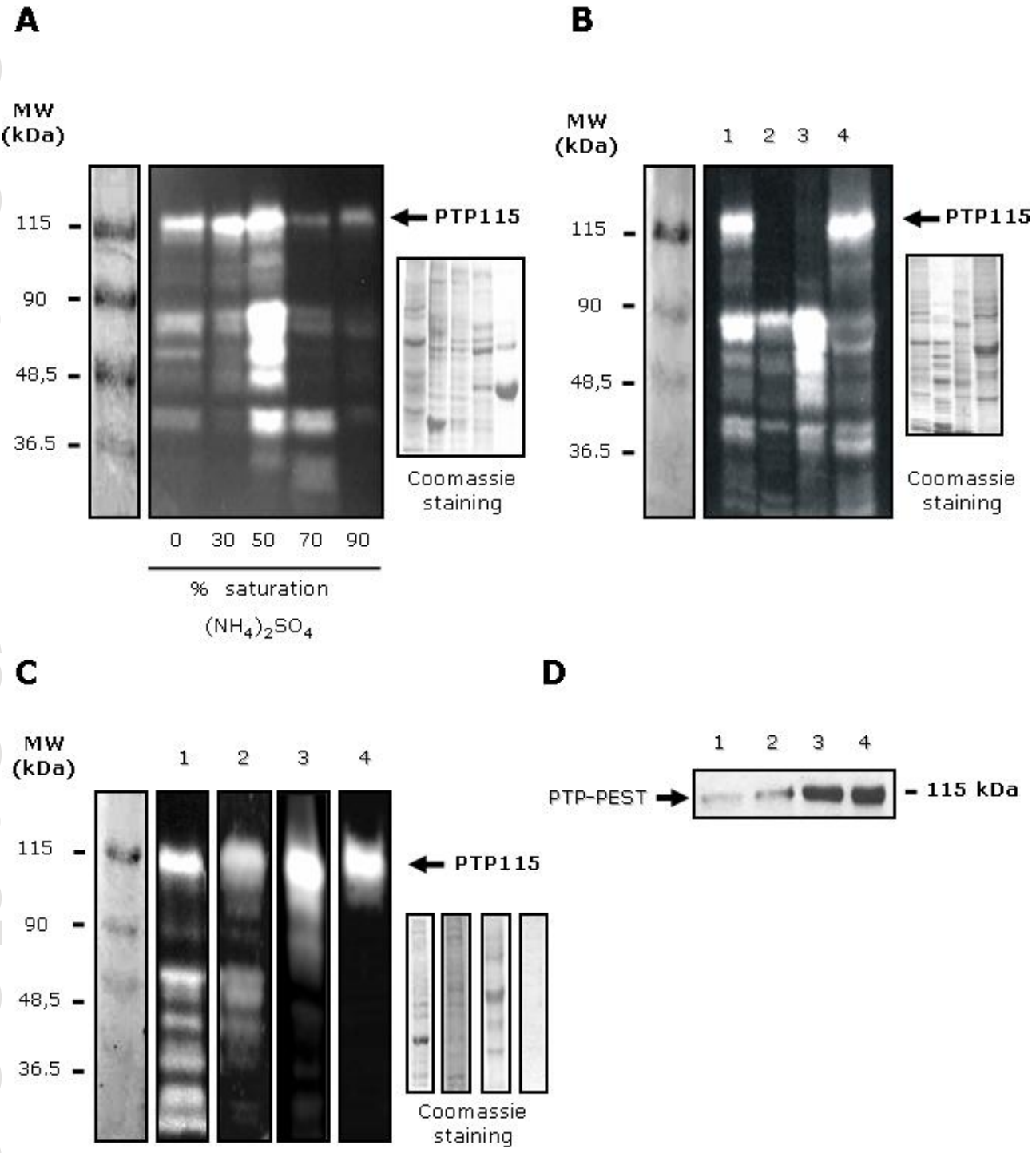

Figure 4

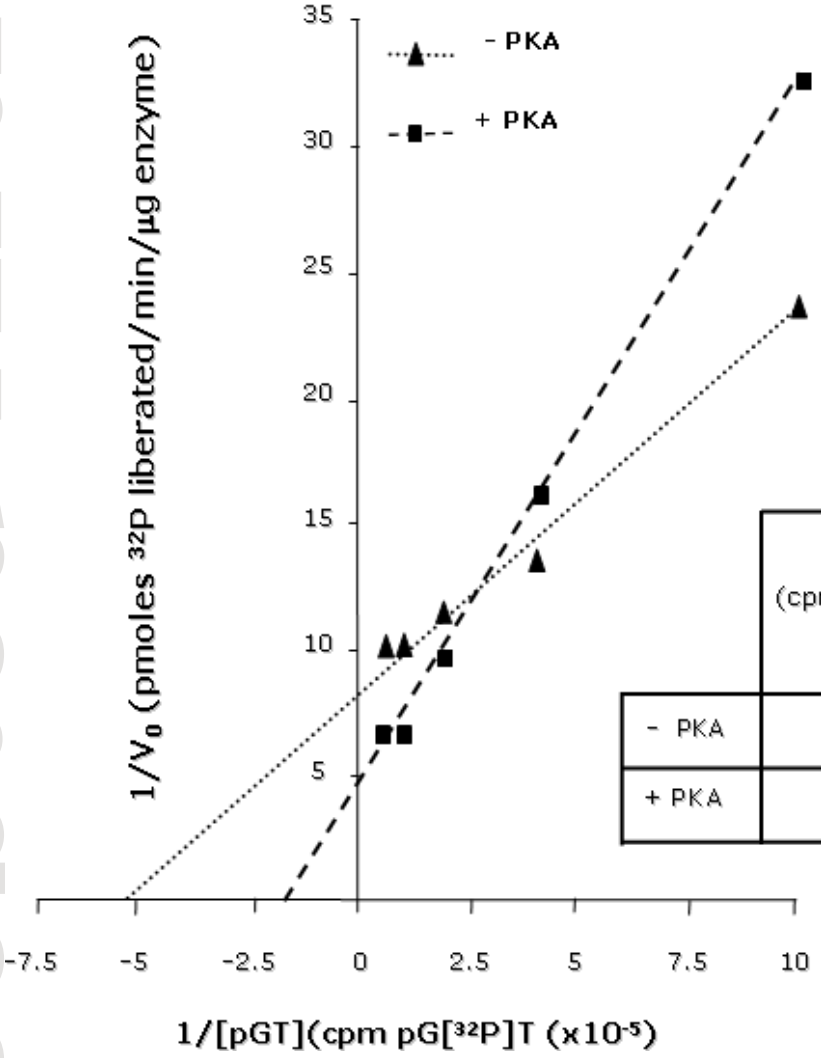

	Km (cpm pG[^{32}P]T)	Vmax (pmoles ^{32}P liberated /min/µg enzyme)
- PKA	19,230	0.132
+ PKA	58, 823	0.212

Figure 5

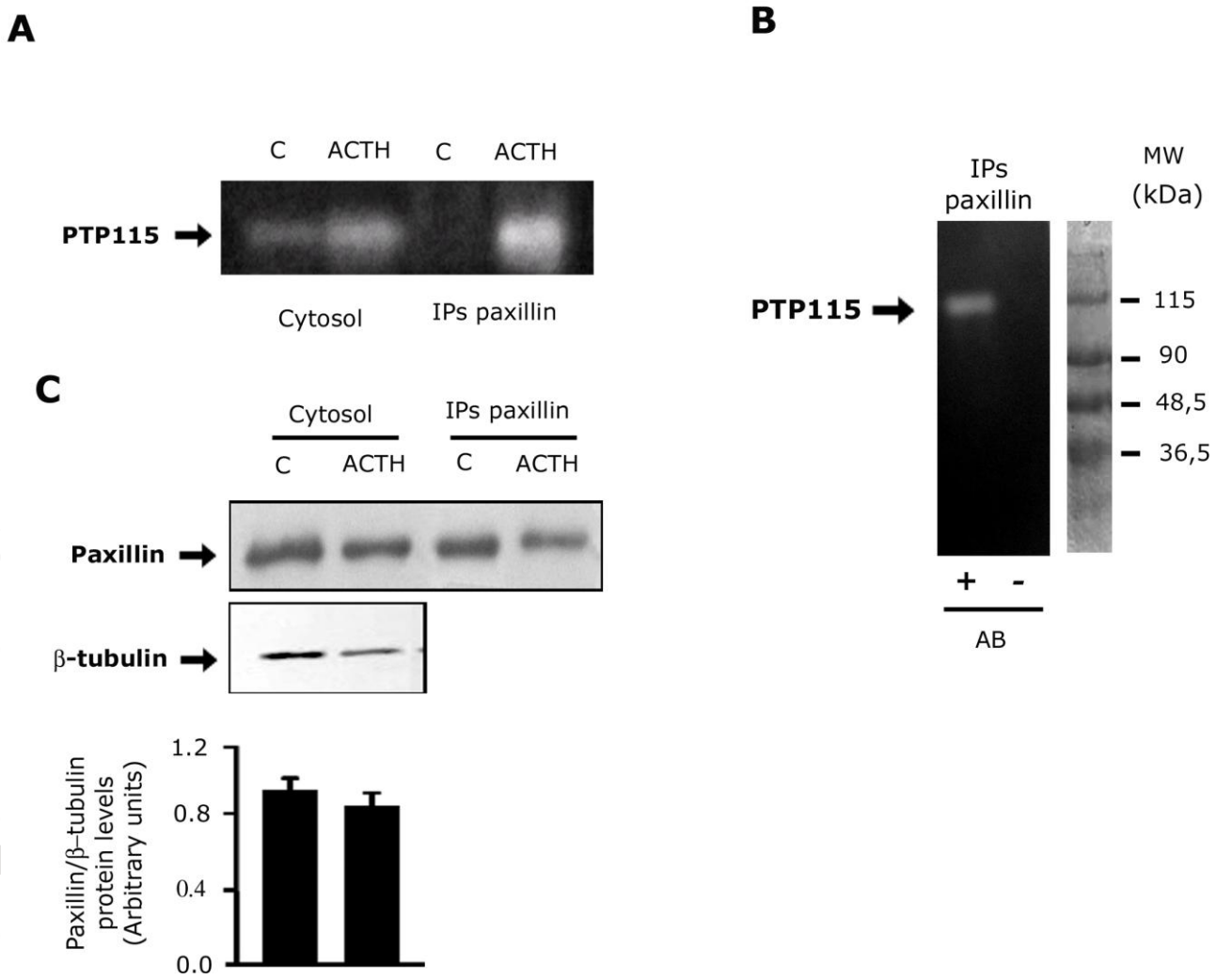

Figure 6

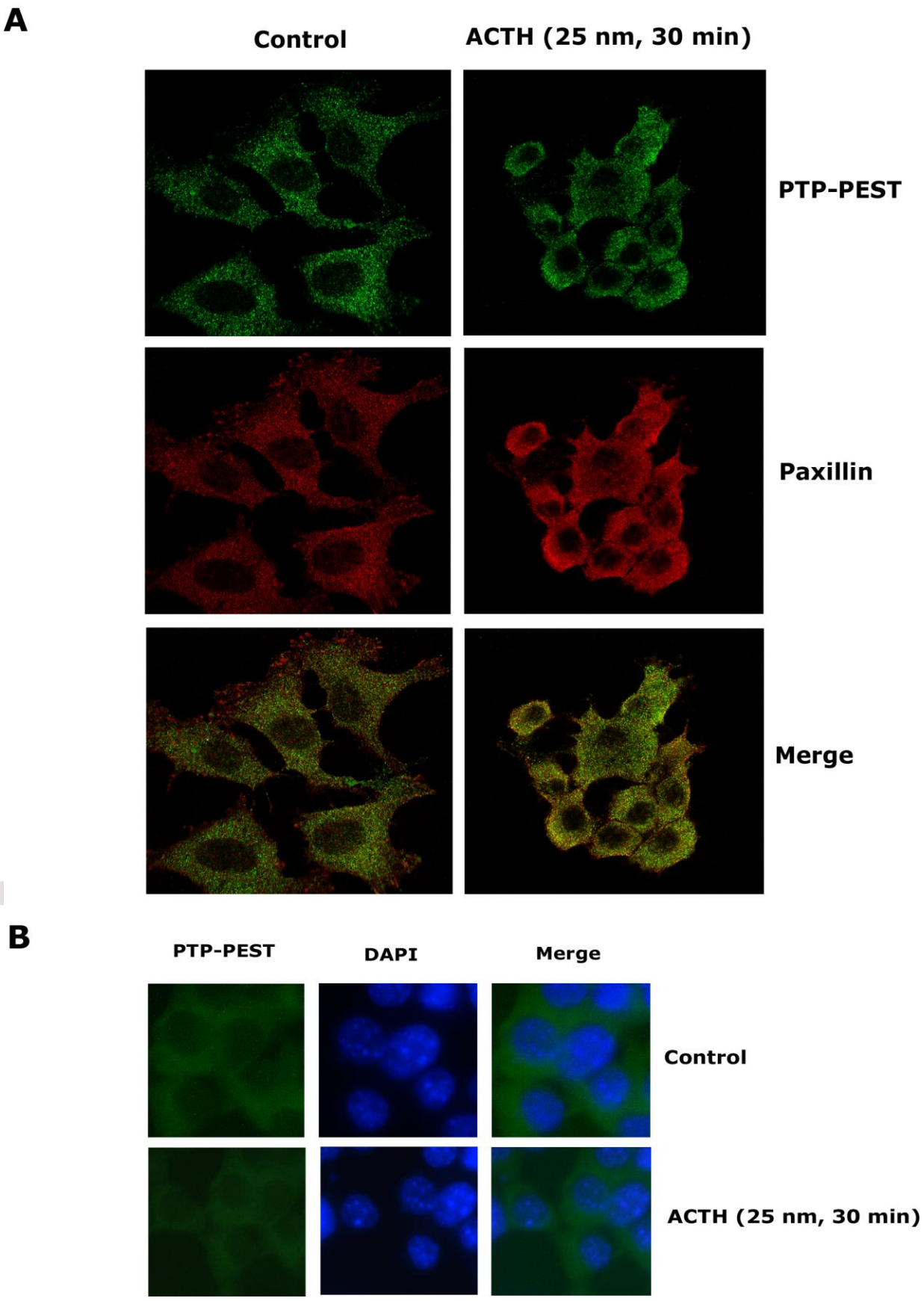

Figure 7